

SEDIMENTARY SIGNATURES OF CYCLIC GROWTH AND DESTRUCTION OF STRATOVOLCANOES: A CASE STUDY FROM MT. TARANAKI, NEW ZEALAND.

Anke V. Zernack, Jonathan N. Procter, Shane J. Cronin

Volcanic Risk Solutions, Institute of Natural Resources, Massey University, Private Bag 11
222, Palmerston North 4442, New Zealand

(a.v.zernack@massey.ac.nz)

ABSTRACT

The long-term behaviour of andesite stratovolcanoes is characterised by a repetition of edifice growth phases followed by collapse. This cyclic pattern represents a natural frequency at varying timescales in the growth dynamics of stratovolcanoes worldwide. Around the >130 ka Mt. Taranaki (Egmont volcano), New Zealand, coastal-cliff successions at 20-40 km distance comprise repeating packages of lithologically and sedimentologically distinctive mass-flow deposits. Varying depositional mechanisms and source properties of these units record growth and collapse cycles of the central edifice. These are used to construct a model for cyclic volcanoclastic sedimentation in the surrounds of stratovolcanoes. During edifice-construction phases, thick packages of tabular, predominantly monolithologic, hyperconcentrated-flow and debris-flow deposits accumulate with intercalated tephra beds. The mass-flow units commonly contain large proportions of fresh pumice or juvenile-lithic andesite. Intervals of quiescence separating eruptive periods are characterised by landscape re-adjustment, accompanied by deposition of fluvial and aeolian sediments, along with steady accretion of medial ash. In contrast, brief episodes of destruction are marked by wide-spread, distinctively clay-rich, polyolithologic debris-avalanche deposits and related marginal debris flow units. The growth stages can be terminated by an eruption-triggered sector collapse, or by external forces once the edifice exceeds a critical stable height or profile (dependent on eruptive style and local geo-tectonic conditions). Once the edifice becomes metastable, regional tectonic

earthquakes or shallow-level intrusion events are likely triggers for collapse. Although the resulting debris avalanches represent the greatest individual hazard from such andesite stratovolcanoes, their frequency is relatively low compared with other types of mass-flows generated during edifice-growth phases. Accurate forecasts of future hazard from mass-flow events are therefore dependent on recognition of both the frequency of a stratovolcano's growth cycle and its current position in that cycle.

Keywords Mt. Taranaki/Egmont, volcanoclastic, debris avalanche, debris flow, lahar, hyperconcentrated flow

1. Introduction

Debris avalanches resulting from the collapse of volcanic edifices have been described at many volcanoes worldwide (e.g. Voight et al., 1981; Crandell et al., 1984; Siebert, 1984; Ui et al., 1986b; Glicken, 1996; Vallance et al., 1995; van Wyk de Vries & Francis, 1997; Capra et al., 2002; Waythomas & Wallace, 2002; Concha-Dimas et al., 2005; Shea et al., 2008) yet from most stratovolcanoes only one major lateral collapse is known, with possible older events being hidden. Repeated debris avalanche events have been inferred from just a few long-lived examples, e.g. St. Augustine (Beget & Kienle, 1992), Colima (Stoops & Sheridan, 1992), Mt. Rainier (Vallance & Scott, 1997), Shiveluch (Belousov et al., 1999), as well as from a number of ocean island volcanoes, e.g. Stromboli (Kokelaar & Romagnoli, 1995; Tibaldi et al., 2001), Reunion (Lenat et al., 1989; Labazuy, 1996), Canary Islands (Holcomb & Searle, 1991; Carracedo, 1994, 1996; Walter & Schmincke, 2002), and Hawaii (Fornari & Campbell, 1987; Moore et al., 1994), which have been studied by oceanographic methods. However, in many of these locations, the oldest units are deeply buried by more recent volcanoclastic deposits, or are only preserved below sea-level. Consequently, reconstruction

of the volcanic history for hazard analysis is usually based on interpretations of the Holocene record (Siebert et al. 1995; Thouret et al. 1995; Scott et al. 1997; Belousov et al. 1999; Waythomas 1999; Waythomas & Miller 1999; Reid et al. 2001). This brief interval may fail to identify longer-term influences on the activity, stability and evolution of stratovolcanoes.

The most complete chronostratigraphic record of volcanic activity and other sedimentary events is recorded in volcanic ring plain successions, which are progressively built up by deposition of syn- and post-eruptive volcanoclastics and minor primary products, as well as reworked deposits (Palmer & Neall, 1991; Smith, 1991; Cronin et al., 1996; Davidson & De Silva, 2000; Donoghue & Neall, 2001; Borgia & van Wyk de Vries, 2003). Hence, in order to reconstruct the eruptive history of a stratovolcano in more detail and to recognise its true hazard potential, it is important to understand the depositional processes that contributed to the construction of the volcanic ring plain

Unusually, at Mt. Taranaki, also known as Egmont volcano, New Zealand, a stratigraphic record is exposed in medial ring-plain successions that span most of the life of the volcano (Neall, 1979). This is due to continuous coastal erosion of the tectonically uplifted Taranaki Peninsula (Pillans, 1994). These circumstances allow the reconstruction of volcanic and other landscape-forming events operating over the life-span of this stratovolcano, based on the correlation of the exposed ring-plain deposits and their sedimentological classification. The unique long-term record of this repeatedly collapsing volcano provides a better understanding of the nature and processes behind the volcano's behaviour and is here used to develop a model of cyclic behaviour and sedimentation that can be applied to stratovolcanoes in general.

2. Mt. Taranaki / Egmont volcano

Mt. Taranaki (2,518 m) has been active for at least 130 ka (Alloway et al., 2005) and represents the youngest expression of andesite volcanism along a NW-SE trending, c. 1.8 Ma

lineament (Neall, 1979). The modern edifice is made up of lavas and pyroclastic deposits that are mostly younger than 14 ka. These represent only a small fraction (c. 12 km³) of the total volume of material erupted (Neall et al., 1986). The volumetrically larger (c. 150 km³) ring-plain surrounding the volcano contains debris-avalanche and other mass-flow as well as fluvial deposits (Fig. 1). At least six debris avalanche deposits were identified previously and attributed to collapses from former edifices (Neall et al., 1986; Alloway et al., 2005). Collapses occurred on different sectors of the cone at different times throughout its history. The only location where debris avalanches and lahars are not deposited is in the north-west sector, where the deeply eroded remnants of Kaitake and Pouakai volcano blocked the flow-paths. The largest known failure produced the Pungarehu Formation, with an onshore volume of c. 7.5 km³ (Ui, 1986a).

FIGURE 1

Debris avalanches at Mt. Taranaki spread out broadly on the gently dissected ring-plain (Fig. 1C) and therefore show distinctive surface geometries and lithofacies distributions (Palmer et al., 1991). They form a characteristic hummocky landscape with the highest density of large hills along the main dispersal axes; these reduce in spatial density and size laterally and with runout distance. Medial sequences are exposed at distances > 20 km from the current summit and onshore deposits are limited to within 40 km.

Palmer and Neall (1991) recognised that these units record large-scale destructional events, in contrast to periods of cone growth, which are represented by lahar (debris flow and hyperconcentrated flow) deposits in medial locations. Based on the dominant lithofacies element, the medial volcanoclastic succession in south-west Taranaki was split into an inferred cone-construction sequence and a sequence representing failure of the edifice.

3. Age and distribution of debris avalanche deposits

Based on new results presented here, along with previous work, there are now at least 13 large debris avalanche deposits identified in the >130 ka record of Mt. Taranaki (Table 1). This implies that major slope failures take place on-average every 10 ka, however, collapse events appear by no means evenly spaced over time. Five collapses are recognised over the last 30 ka where stratigraphic records are more complete. The oldest debris avalanche deposit (Mangati) identified in cliff sections at the north-eastern coast is most likely derived from Mt. Taranaki but due to limited outcrops an origin from Pouakai Volcano cannot be ruled out beyond doubt.

TABLE 1

In this study, radiocarbon ages were collected for the youngest debris avalanche deposits from ripped-up wood and intercalating peat layers (Table 2). The age of older units was estimated from their stratigraphic position in relation to mapped marine terraces and tephrochronology (Pillans, 1983; Neall, 1986; Alloway, 1989; Alloway et al., 2005). The number of debris avalanche events so far identified is likely to be a minimum. Other units may be buried beneath young ring-plain sediments, in particular to the east of the volcano, where outcrops are rare, and to the west where no significant uplift has occurred to elevate older parts of the succession. Apparent gaps in the reconstructed volcanic history may therefore simply reflect the limits of available stratigraphic record. In addition, the true run-out distances of the Taranaki debris avalanches are difficult to estimate, although their deposits extend at least 25 km (some more than 45 km) onshore and a minimum of a further 6 km offshore (Alloway et al., 2005).

TABLE 2

Failures have occurred on similar sectors of the edifice during certain time periods, indicating that different parts of the edifice were more unstable and thus vulnerable to collapse at different times throughout the volcanic history. This may indicate that the direction of collapse was influenced by internal and/or external processes, such as stress regimes within

the volcano, the regional tectonic stress field, or the geometry of the contact with the subvolcanic basement (Siebert, 1984; Vallance et al., 1995; van Wyk de Vries & Borgia, 1996; Lagmay et al., 2000).

4. Sedimentary characteristics of volcanoclastic and reworked epiclastic deposits

Volcanoclastic deposition at Mt. Taranaki has formed a surrounding ring-plain which extends 25-45 km onshore from the current summit. Sequences along the northern and southern Taranaki coast (Fig. 1C) represent a cross-section through medial ring-plain settings. The exposed units show a wide range of lithologies, which reflect the whole spectrum of sediment-water flow from highly concentrated debris flow to dilute stream flow. Based on their different sedimentological characteristics, the deposits were classified into volcanoclastic, fluvial and aeolian facies. Distinction criteria and main deposit features are summarised in Table 3 at the end of this section.

4.1. Debris avalanche and related debris flow deposits

Major sector or cone collapses at Mt. Taranaki produced debris avalanches that flowed onto gently dissected terrain. Two distinctive types of debris avalanche deposits occur: a dominant “granular-type” is distinguished from one “cohesive-type” unit, i.e. the Otakeho debris avalanche deposit which contains significantly higher matrix clay contents.

Taranaki debris avalanches were effectively unconfined and formed broad deposit fans. This resulted in the development of three distinct lithofacies (Palmer & Neall, 1991) with distributions differing from valley-confined debris avalanches. Axial-A facies forms lobes near source and is dominated by brecciated, self-supporting megaclasts in <30% sandy matrix and a hummocky surface expression with closely spaced, large mounds. Interclast matrix-rich axial-B facies is also attributed to the avalanche phase of the landslide and characterised by

cracked and shattered clasts and megaclasts, few rip-up clasts, 30-90% interclast matrix, and smaller, more widely spaced mounds. Towards the margins it grades into thinner, matrix-supported (> 90%) debris-flow deposits that show a progressive decrease in primary clasts and an increase in secondary components, a relatively planar surface and only scattered low mounds (marginal facies). In medial areas >25 km from source, only major debris avalanches produced deposits of axial-B facies while those generated from smaller collapse events had already transformed into run-out debris flows.

In general, Taranaki debris avalanche deposits drape broad areas of the landscape, displaying a typically sharp, but non-erosive contact in medial areas and filling former depressions or channels often over 5 m in depth. Evidence of shearing and in-situ deformation of the underlying strata is rare and was only observed in the run-out facies of the > 250 ka (Gaylord et al., 1993) Maitahi debris avalanche deposit from the neighbouring Pouakai Volcano.

A distinct basal layer of subangular to mostly rounded cobbles and boulders occurs in some deposits (Fig. 2F), which may indicate where the debris avalanche incorporated particles from river/stream beds or coastal areas. Many deposits locally have a dense-clast rich basal part that is greenish-brown in colour. They also often show a yellow-brownish top half which contains correspondingly less dense clasts and a higher percentage of lighter clasts and matrix components.

FIGURE 2

Granular type debris avalanche deposits

The granular type is very coarse, poly lithologic, very poorly sorted, and non-stratified (Fig. 2A). The deposits contain primary and secondary clasts as well as megaclasts in a matrix, which makes up > 80% of the deposit and consists of small volcanic fragments and individual crystals from clay-size to very coarse sand. A major primary component are disaggregated clasts, which can be up to 2 m in diameter and range in lithology from fragments of lava

flows/domes, scoria and pumice to various types of xenoliths. Larger lava blocks are often fractured and/or show jigsaw cracks (Fig. 2B) with different openings, some containing matrix (cf. Ui et al., 1986a). Matrix is found to have infiltrated the cracks, indicating that they widened during transport, which allowed matrix to intrude into the developing gaps. This fracturing process gradually split the block into several smaller blocks and isolated clasts (Ui et al., 1986a). The fractured lava blocks are typically clustered and surrounded by smaller monolithologic clasts in the matrix.

Megaclasts were defined by Palmer et al. (1991) as “all components of the deposit > 1 m maximum size that are bounded by an outer surface and show an internal lithological homogeneity”. Here megaclast is size-independent and refers to relatively intact fragments of original edifice strata, which can be strongly brecciated or stratified and are bounded by an outer surface. In the coastal area they range in size from c. 0.2 m to 10 m and rarely up to 50 m (Fig. 2C) and include “brecciated clasts” (Fig. 2D), i.e. intensely brecciated single rock types < 1 m in diameter (Palmer et al., 1991). Most megaclasts, in particular the smaller ones, are rounded and coated by a several cm-thick rim of finer-grained inter-clast matrix. Lithologically homogeneous megaclasts composed of brecciated grey to dark grey basaltic andesite or andesite lava are the most common type. The lava is intensely shattered and is fractured into numerous irregular clasts, which range in size from a few mm to tens of cm, forming a characteristic jigsaw pattern (Ui et al., 1986a). Clusters of smaller brecciated megaclasts of different sizes are often found in proximity to larger ones of identical lithology, indicating that these split up into smaller aggregates during transport. They continue to disaggregate until their fractured components are dispersed as discrete clasts in the matrix (Alloway et al., 2005). Stratified megaclasts that preserve the original stratigraphy and primary layering are rare in the studied medial debris avalanche deposits. They are more common closer to source and are a significant component of Axial-A facies (Palmer et al., 1991).

With distance from source, the flows apparently incorporated an increasing amount of secondary components during transport (Palmer et al., 1991; Alloway et al., 2005). The most common rip-up clasts are fragments of the underlying strata, including older debris avalanche, debris flow and hyperconcentrated flow deposits, soil and peat beds with or without intercalated tephra layers, fluvial and aeolian sediments, as well as individual subrounded to rounded fluvial clasts (Fig. 2E). Some debris avalanche units contain large quantities of entrained branches and tree stumps of a variety of lowland species, reflecting a warm climate and dense vegetation at the time of their deposition. The occurrence of small, typically < 1.5 m, rounded and often strongly deformed ripped-up pieces of mud- and sandstone within the oldest units indicate that the earliest debris avalanches at least partly travelled across exposed Tertiary basement. Fragments of Tertiary rocks are absent in the younger units, suggesting that they moved across a progressively thickening volcanoclastic substrate. The granular-type debris avalanche deposits show interclast matrix-rich axial-B facies close to the axis of distribution and a maximum thickness of c. 8 m with the exception of the Pungarehu Formation, which exceeds 15 m at medial coastal locations (Palmer et al., 1991). The lateral transition into matrix-supported marginal facies is marked by a decrease in overall thickness and clast size, an increase of matrix relative to clasts, decreasing abundance and size of primary megaclasts, and an increase in secondary clasts. Number and size of clasts and rip-up clasts continuously decrease towards the marginal and distal limits of the deposits, until they become a relatively homogeneous mixture of clay-rich matrix and sparser gravel- to sand-sized volcanic particles. The deposits wedge out abruptly at their margins from <0.5 to 0 m within 10 m.

Cohesive type debris avalanche deposits

The cohesive type is poorly sorted, poly lithologic, contains small (<5-10 cm in diameter) and completely disaggregated clasts in >95% allophane-rich matrix (Fig. 3A). Further components

are abundant large logs and wood fragments as well as small ripped-up pieces of underlying soil and tephra beds, few brecciated clasts and rare, small rounded megaclasts (Figs. 3B-D). The deposits are more wide-spread than the granular type but of relatively constant thickness (typically 2-3 m) with a maximum observed medial thickness of 4 m. In the coastal areas, only the marginal facies is exposed, which shows a slight increase in clast abundance and size (15-20 cm in diameter) close to the main dispersal axis.

FIGURE 3

4.2. Channelised debris-flow and associated overbank deposits

Where lahars were confined to pre-existing river channels they formed very coarse, very poorly to extremely poorly sorted, clast-supported, massive deposits with little sandy matrix. These are non-graded, lack internal stratification and often developed a thin matrix-supported base. Boulders are rounded to angular and can be more than 2 m in diameter (Fig. 4A). Large angular-subangular boulders could be derived from older debris avalanche deposits while the well-rounded clasts were probably picked up from the underlying river bed. Some units grade upward into moderately to poorly sorted, bedded, sandy hyperconcentrated flow deposits. This has been described elsewhere and interpreted by several authors (c.f., Pierson & Scott, 1985; Smith, 1986; Cronin et al., 2000) as reflecting deposition from the dilute waning stage of flow. Intercalated lenses of bedded and cross-bedded sands fill small surface channels that represent rapid post-depositional reworking of the deposit by fluvial processes. Typically, these channelised debris flow deposits are lenticular with erosive basal and marginal contacts cut deeply into the underlying and abutting deposits. Individual units are up to 5 m thick but extend only several tens of metres laterally before grading into thinner, more wide-spread overbank deposits (Fig. 4B-D). These tabular, overbank units drape the substrate with no erosional contacts and extend up to 250 m from the channel margin. They are better sorted than the channel facies and consist primarily of fine pebbly sands. The deposits become

progressively finer-grained and better sorted with distance laterally from the channel margins, showing in outer reaches faint internal stratification with thin horizontal or very low-angle cross beds.

FIGURE 4

4.3. Sheet-like hyperconcentrated-flow deposits

Distinct from the lahar overbank facies deposits are more wide-spread, pebbly sand-dominated tabular units that are interpreted to have been emplaced by hyperconcentrated flows with a wide range of sediment/water ratios and thus diverse flow behaviour. These deposits encompass features such as poor to moderate sorting, massive or bedded, reverse-to-normal, normal or non-graded, tabular with continuous straight boundaries, or lenticular with erosive basal contacts. They contain mostly angular, predominantly monolithologic clasts. Monolithologic pumice and scoria-rich flows (Fig. 5A) are similar to those generated from remobilised tephra fall following explosive subplinian eruptions (c.f., Cronin et al., 1997). Flows dominated by dense andesite clasts (Fig. 5B) appear to represent the reworking of dome-collapse block-and-ash-flows which are common in the volcanic history of Mt. Taranaki (Platz et al., 2007). Polyolithologic flows (Fig. 5C) were probably not directly related to an eruption but represent the run-out of lahars and reworking floods. The deposits can be traced up to 2.5 km in lateral exposure and thicken in small channels but do not show distinct transitions from confined coarse debris flow to overbank facies.

FIGURE 5

Coarser units, produced by sediment-rich, high-competence flows transitional between debris and hyperconcentrated flow often show reverse-to-normal grading. The deposits are typically 0.4-0.6 m and rarely up to 1.5 m thick, consist of an inversely graded, fine-grained base and a coarse main body, which grades into a finer-grained top (Fig. 6A). The basal unit comprises fine angular to subangular pebbles and sand, can be faintly bedded and is sometimes

underlain by a thin (c. 1 cm), well-sorted layer of fine to coarse sand. The overlying main part of the deposit is coarse, massive, poorly sorted with angular to subrounded, large pebble to small cobble-sized clasts in a sandy matrix and often shows normal grading into a finer-grained, bedded pebbly sandy top. These characteristics reflect the gradational vertical transition from a basal hyperconcentrated flow deposit upward to a debris flow unit (Pierson & Scott, 1985; Cronin et al., 1999). The basal layer indicates passage of a watery front-wave with competence increasing over time. The following main body of the flow produces the overlying debris flow unit. With increasing dilution downstream the basal layer thickens, while the overlying debris flow portion thins (c.f., Scott, 1988; Scott et al., 1995). The top part of the deposit can be fine-grained and bedded, representing the transition to more dilute flow and decreasing energy. Typically, a thin silty layer develops on top after deposition due to settling and dewatering of the sediment (cf., Cronin et al., 2000).

Non-graded, poorly sorted, coarse deposits with pebble- to boulder-sized clasts in a sandy matrix occur and likely represent the most concentrated of these non-cohesive debris flow/hyperconcentrated flow deposits (Fig. 6B). They lack internal stratification, are tabular and non-erosive or lenticular with scoured basal contacts. Individual units can be up to 1.7 m thick.

FIGURE 6

Thinner and finer-grained sediments consisting of pebbly sands are interbedded. These units are moderately to poorly sorted, show weak grain-size defined bedding on a cm to 20 cm scale (Fig. 6C) and commonly contain scattered clasts of cobble- and up to boulder-size. The basal contact of these deposits can be erosive or non-scoured. Upward-decreasing grain-size, better sorting and more distinct bedding indicate transition to higher water contents and a lower sediment concentration of the transport medium. The resulting deposits are moderately sorted and show horizontal lamination of fine and coarse sands with the occasional

occurrence of isolated pebble- and rare cobble-sized clasts. The deposits are often lenticular with a wavy, erosive base.

Fine-grained, pumice-rich hyperconcentrated deposits can show pumice ‘trains’ and discontinuous beds of coarser particles aligned parallel to the depositional surface and bedding (Fig. 6C). Clustering of small pebbles in front of larger clasts that represented a barrier during flow also occurs (Fig. 6D). The deposits are typically 0.2-0.5 m thick but can be as thick as c. 2 m (faintly bedded coarser units) or 1.2 m thickness (well-bedded fine-grained units). Post-depositional deformation and dewatering structures are common, such as dish and pillar structures (Fig. 6E) and load-induced flame structures (Fig. 6 F). This implies that stacks of several units were probably emplaced in rapid succession.

4.4. Transition hyperconcentrated flow / stream flow deposit

Deposits representing runout and margins of the hyperconcentrated flows are moderate to well-sorted, fine- to coarse-grained sands, typically with low-angle cross-bedding or strongly developed horizontal to wavy bedding (Fig. 7A). Lenses of cross-bedded fine sands and rounded pumice lapilli are common. The deposits are lenticular with very erosive basal contacts and often form steep, overlapping channels (Fig. 7B). Their thickness ranges from a few cm to 0.5 m.

FIGURE 7

4.5. Fluvial deposits

Different types of fluvial reworked equivalents of the volcaniclastic units above occur in the medial sequences. The most common deposits consist of alternating lenses of well-sorted fine to coarse sands and moderately to poorly sorted, rounded to subrounded pebbles and sands separated by low-angle erosion surfaces (Fig. 8A, C). Individual sand beds are typically a few mm to 1 cm thick, while pebble layers are 1 to 10 cm thick. The deposits show horizontal

lamination (sands), low-angle cross-stratification and prominent scour-fill cross-bedding. Contacts to the underlying deposits are erosive. The sequences are up to 4 m thick and highly localised in distribution, but can laterally extent up to 150 m. Complex sequences of overlapping channels that cover wider stretches of coastline reflect the locations of larger, long-lived river systems. These accumulated massive, sometimes >10 m thick, aggradational series of more poorly sorted sediments, made up of rounded volcanic clasts ranging from pebble- to boulder-size with intercalated cross-bedded lenses of small pebbles and sand (Fig. 8B, D).

FIGURE 8

4.6. Aeolian deposits

In some areas, dune sands occur, consisting of alternating thin (0.5-1 cm) beds of dark grey, very well-sorted fine sands that are rich in dark, mafic, heavy minerals (i.e. ferromagnesian and titanomagnetite minerals) and thicker (up to 2 cm) beds of coarser, light yellow to brownish, well-sorted sands (Fig. 9A). Individual sets of dune sands are tens of cm to c. 1.5 m thick and show planar or high-angle cross-stratification (Fig. 9B). They form sequences that can be more than 12 m thick and are typically interbedded with thin (5-10 cm thick) organic-rich peat layers or iron-stained, weakly developed tephric soils as well as a number of sandy hyperconcentrated sheet-flow deposits. Intercalated coarser beds of rounded pumice lapilli and the absence of interbedded primary tephra layers indicate rapid saltation and redeposition of tephra within this area of aeolian reworking. Aerially exposed volcanoclastic and fluvial deposits provided further source material for dune sand formation.

FIGURE 9

5. Volcanoclastic lithofacies associations

Medial ring-plain sequences are built of at least six different lithofacies elements that correspond to a range of transport and emplacement modes as well as various depositional environments.

5.1. Debris avalanche-dominated sequences

The gently dissected, flat nature of the ring-plain around Mount Taranaki resulted in relatively unconfined, very thick, laterally extensive debris avalanche and related debris flow deposits (cf. Table 1). Emplacement of these changed the focus of sedimentation dramatically, with most deposition taking place beside the new landscape-forming deposits until the next large landscape-draping flow occurred. Hence sequences of stacked debris avalanche and debris flow units are formed with little accumulation of other deposits between them, apart from tephric soils and peats (Figs. 10A and 11A). The collapse events also significantly modified the pre-existing drainage system, with debris avalanche units burying older river systems. Re-establishment of the drainage system is indicated by deep channels that were cut into and beside the avalanche deposits (Fig. 10B). These accumulated coarse reworked material from the debris avalanche units as well as being partially filled by later debris flow deposits. Smaller stream systems reworked the surface of the avalanche to produce minor localised cross-bedded fluvial gravels and sands.

FIGURE 10

5.2. Paleochannel-systems

Ring-plain locations record a network of separate and overlapping, laterally migrating paleochannels that were repeatedly infilled. These represented major flow paths for coarse, voluminous debris flows, which in most cases eroded the fluvial and underlying deposits and filled the central channel area. These are separated from each other by unconformities filled with thin cross-bedded lenses of sand, representing reworking by fluvial processes between

lahar events. The central channel area can be as thick as 10 m but typically extends only 15-60 m laterally (Fig. 10B). The lateral transition from channel area to floodplain is marked by a change into thinner, finer-grained, tabular, hyperconcentrated flow deposits. Vertically, the sequences typically show a fining-upward to a series of thin hyperconcentrated deposits emplaced in shallow, broad channels (Fig. 11B). Interbedded fluvial sediments represent local re-establishment of paleo-streams and fluvial reworking.

FIGURE 11

5.3. Sequence dominated by sheet-flow deposits

Hyperconcentrated and transitional hyperconcentrated-debris flow facies associations are an important architectural element in broad flat interfluve areas of medial ring-plain locations. They occur as single depositional units of varying thickness or as massive series, forming sequences up to 15 m thick (Fig. 10C). Their wide range of sedimentary characteristics is a result of relatively minor variations in sediment concentration and lithology. Short breaks in volcanoclastic sedimentation are characterised by tephric soil and/or peat formation and localised fluvial deposition in paleo-stream locations (Fig. 11C). These tabular units can be traced over lateral distances of up to 2.5 km. In other cases erosional surfaces and deep channels give them a seemingly lenticular appearance.

5.4. Fluvial facies associations

Fluvial deposits occur throughout all successions, representing periods of stream and river reworking and re-establishment. They are typically highly localised and show bedding features that represent at least two different settings. The first is more common and characterised by relatively thin bedding, low relief of scours and low amplitude of cross-stratification, which suggests deposition by shallow, rapid stream flow in broad, braided

channels (Smith, 1987). Thicker aggradational series of mostly horizontally bedded fluvial gravel and sand are rare and steadily accumulated in deeper, wide river channels.

5.5. Dune sands

Cross-bedded aeolian sands occur as sequences of > 12 m thick (Fig. 11D) and are exposed over a wide stretch of coastline (> 15 km). In some areas they are interbedded with thin (< 0.5 m thick) single or multiple volcanoclastic mass flow deposits or localised fluvial sediments. The dune sands accumulated during cool as well as mild climates indicated by different types of intercalated paleosols, i.e. tephric soils as well as peat beds. The considerable thickness, wide distribution, intercalated hyperconcentrated-flow deposits, numerous thin peat beds, iron-stained weathering horizons and weakly developed soils in the tops of individual dune sets indicate that the dune sands accumulated over a long period of time. It is unlikely that they correspond to an earlier period of cold-climate aeolian redeposition such as the Katikara Formation that accumulated in north-west Taranaki at the end of the last Glaciation (Alloway, 1989). Instead, they are believed to have formed in a relatively undisturbed near-coastal environment since they are similar in extent and characteristics to present-day near-shore dune fields. Such an incursion of sand dunes is likely to have been triggered by one of the higher sea level stands of the last Interglacial. Based on their stratigraphic position the sands are correlated with MISS 5a, giving an approximate age of < 80 ka.

5.6. Soil- and peat-dominated sequences

Paleosol-dominated stratigraphic intervals represent areas with relatively low sedimentation rates and periods of landscape stability. These are characterised by accumulation of thick layers of medial ash or peat and the preservation of (typically < 2cm) thick tephra beds. Cold climate paleosol sequences consist of interbedded volcanic (loess and tephra) soils as well as tephra beds and can be as thick as 2.5 m. Peat-dominated sequences up to 1.5 m thick, formed

in areas of poor drainage and are intercalated with medial ash and tephras. In some areas, the soil formation process is interrupted by infrequent emplacement events of single debris or hyperconcentrated flow units.

7. Volcanic cycles

These lithotype associations can be linked to specific phases within a repeating pattern of deposition, which are here used to develop a model for cyclic volcanoclastic sedimentation in the surrounds of unstable stratovolcanoes (Fig. 12).

FIGURE 12

A generalised volcanic cycle at Mt. Taranaki arbitrarily starts after the destruction of large portions of the edifice by collapse. The long-term regeneration of the deeply scarred edifice begins with small-scale pyroclastic eruptions, dome-building and localised lava flows, the background activity typical of this centre (Platz et al., 2007). Medial areas accumulate thick tephric soils or peat with interbedded tephra layers that reflect the proximal activity. Mass-flows produced during this period are mostly restricted to proximal areas due to the lower elevation of the source area. With increasing height of the growing edifice, eruption-generated mass-flows start to reach greater distances of >25 km. Subsequently, medial accumulation is characterised by massive sequences of mainly monolithologic debris-flow and hyperconcentrated-flow deposits with intercalated tephra beds. These are sheet-like on broad terraces and coastal planes or confined to channels where the landscape has been incised by rivers and streams (Procter et al., 2008, this volume). Volcanic activity is not constant and deposition loci change, resulting in frequent periods of apparent quiescence for variable sectors of the ring plain. These are recorded by soil, medial ash, or peat accumulation, along with landscape adjustment through fluvial and aeolian processes.

The similar extent and run-out distance of the Taranaki debris avalanches suggest that the edifice is regenerated to a similar size before it collapses again. Edifice growth is ultimately limited to a critical point at which its structure becomes sufficiently unstable that even a weak disturbance may cause it to fail. Although, a strong dynamic or magmatic event can trigger collapse of a more stable edifice before a critical height and/or slope is attained (Belousov et al., 1999; Siebert, 1984). The volcanic cycle is closed with a major sector or cone collapse, represented by debris avalanche and long run-out debris flows in medial areas. Major debris avalanches bury extensive areas of the ring-plain and reshape the landscape. They significantly modify the drainage system and change the focus of sedimentation before and after the collapse.

8. Discussion

The characteristics and sedimentary signatures of a volcanic cycle are controlled by a range of internal and external factors.

8.1. Factors leading to edifice instability

Various structural, magmatic and external processes can lead to the increasing instability of a volcanic edifice (Voight et al., 1981; Siebert, 1984; Voight & Elsworth, 1997; McGuire, 2003). A combination of processes has contributed to an inherently unstable structure of present and proto Mt. Taranaki edifices. This is mostly a result of a high content of unconsolidated pyroclastic and volcanoclastic deposits (cf. Siebert, 1984; Vallance et al., 1995), interbedded with lava flows. Megaclasts of intact, layered fragments of edifice strata within the debris avalanches suggest a similar structure for proto-edifices (Neall et al., 1986). Another important structural factor at Mt. Taranaki is the development of steep upper slopes (cf. Siebert, 1984; Beget & Kienle, 1992). The absence of hydrothermally altered components

within the Taranaki debris avalanche deposits indicates that hydrothermal processes did not affect large parts of the edifice as has been observed at other volcanoes (cf. Siebert et al., 1987; Lopez & Williams, 1993; Vallance & Scott, 1997; Voight & Elsworth, 1997). Instead, hydrothermal alteration was probably restricted to the area around the central conduit, leading to a progressively weaker core. Further factors that are recognised to contribute to the instability of volcanoes are their growth on a sloping or weak substrate (Wooller et al., 2004; Carrasco-Nunez et al., 2006), subsidence or uplift of the sub-volcanic basement (Firth et al., 1996; McGuire, 2003) as well as frequent tectonic activity (Francis & Self, 1987). These processes also play an important role in Taranaki where the sub-volcanic basement consists of a Tertiary marine-basin sequence of dominantly poorly consolidated mudstone with interbedded sandstone (Kamp et al., 2004). The substrate is cut by several Quaternary and active faults, some of which extend through the modern edifice (Neall, 1979; Alloway, 1989; Sherburn & White, 2006). Structural alignments, i.e. the SSE migration of the Taranaki volcanoes and the younger N-S alignment of Mt. Taranaki summit, Fanthams Peak and several lava domes (< 3 ka) (Neall 1971; Neall et al., 1986) reflect the more recent tectonic stress field (Sherburn & White, 2006) and might have also contributed to the instability of the volcano (cf. Vallance et al., 1995). The high annual precipitation in Taranaki (> 8 m rainfall per year on the north flank of the volcano) is likely to cause saturation of the porous deposits that build up the edifice, enhance alteration and eventually weakening of the rocks (Scott et al., 2005; Carrasco-Nunez et al., 2006). It is not known in which way the global climatic changes of the last 130 kyr affected Mt. Taranaki because no correlation between edifice failures and abrupt climate changes could be found as was postulated by Capra (2006). Evidence of buttressing and gravitational spreading (cf. Borgia, 1994; Van Wyk de Vries & Francis, 1997; Borgia & van Wyk de Vries, 2003) is absent.

In addition to the above described slow processes that lead to progressive instability of the edifice, magmatic processes can have similar effects on a much shorter time-scale. The

intrusion of fresh magma can result in oversteepening and lateral displacement of the flank, as occurred during the 1980 eruption of Mount St. Helens (Voight et al., 1981), as well as fracturing and pore-fluid pressure enhancement within the edifice (Elsworth & Voight, 1996). A change in the magma composition can also influence edifice stability, like at Shiveluch volcano where an abrupt shift to a higher SiO₂-content of the erupting magma changed the predominant eruptive style to the production of lava domes (Belousov et al., 1999).

8.2. *Trigger mechanisms*

The sedimentary signatures of individual volcanic cycles at repetitively collapsing volcanoes are also controlled by the process causing edifice destruction. Bezymianny-type failures, associated with intrusion of fresh magma (Siebert et al., 1987) can be accompanied by magmatic activity, or trigger explosive eruptions. Thus, regeneration of the edifice starts immediately after its destruction with growth of a new lava dome in the amphitheatre, e.g. St. Augustine (Beget & Kienle, 1992), or with a Plinian eruption followed by lava dome formation, e.g. Mount St. Helens and Shiveluch (Lipman & Mullineaux, 1981; Bogoyavlenskaya et al., 1985; Belousov et al., 1999). In contrast, Bandai-type collapse events (Siebert et al., 1987) are associated with solely phreatic eruptions which cease after debris avalanche generation. Unzen-type slope failures occur without any volcanic activity and are triggered by tectonic earthquakes like nonvolcanic landslides (Siebert et al., 1987).

The trigger mechanism of failures at Mt. Taranaki is not known except for the Ngaere event which Alloway et al. (2005) postulated as being of Bezymianny-type. In contrast, there is no evidence to indicate that magmatic activity initiated or immediately followed the other identified edifice failures. However, the large volume of the 80-35 ka southern debris avalanches and a high content of pumice clasts suggest that they were generated during periods of intensified explosive magmatic activity. The derivation of large amounts of pumice from incorporation of substrate or cutting of voluminous pumice deposits by the failure (van

Wyk de Vries et al., 2001, Shea et al., 2008) is unlikely at Taranaki due to the absence of ignimbrites and the typically small size ($< 1 \text{ km}^3$) of eruptions (Alloway et al., 1995). Direct evidence such as blast deposits and tephra layers associated with debris avalanches is otherwise absent, due to distance from source, prevailing (north-east) wind direction as well as erosion. Tectonic triggers such as large-scale fault movements or gravitational settling-related faulting may represent significant triggering mechanisms once the volcano reaches a metastable height. In addition, environmental factors such as high-intensity rainstorms which can cause a reduction in strength of the edifice due to saturation (McGuire, 2003; Scott et al., 2005; Carrasco-Nunez et al., 2006) could have initiated smaller collapse events.

8.3. Frequency of growth and collapse cycles

The frequency of growth and collapse at a stratovolcano is strongly influenced by the magma supply and the magma ascent rate, which determine the repose times between eruptions and the time it takes to (re)build an edifice. Very high lava effusion rates at Mount St. Augustine, for example, are responsible for rapid regeneration of the edifice after a collapse and recurrence of large debris avalanches approximately every 150-200 years (Beget & Kienle, 1992). A similar conclusion is reached for Shiveluch Volcano, which produced at least 8 debris avalanches in the last 10 ka (Belousov et al., 1999). The averaged 10 ka between major collapses at Mt Taranaki suggest slower growth phases, and overall lower magma recharge rates. The apparent increase in debris-avalanche abundance in the recent record, may have a number of causes, including: a change in magma composition or eruptive style (Belousov et al., 1999), an increase of the magma supply rate (Beget & Kienle, 1992; Belousov et al., 1999), progressive weakening of the core due to hydrothermal alteration around the conduit (Vallance & Scott, 1997; van Wyk de Vries et al., 2000) or persistent dike intrusion (Siebert, 1984). Structural aspects such as regrowth of the edifice on former scars seem to have strongly added to the increasing instability and, together with major climate changes, could be

responsible for a higher frequency of collapses. Furthermore, a gradual shift to more evolved high-K magma composition (Price et al., 1999) may have resulted in the extrusion of more viscous andesite and basaltic-andesite lavas, which presumably produced steeper upper slopes and a higher percentage of lava domes than in the early history of the volcano.

8.4. Type of products/eruptive style

The predominant eruptive style during edifice-building periods may also vary between volcanoes or even between cycles on a single volcano. It is recorded in the clast assemblages of long run-out debris- and hyperconcentrated-flow deposits, which are typically generated in response to a high sediment supply during or after eruptive activity. At Mt. Taranaki some growth phases are characterised by pumice-dominated lahars and tephra layers indicating vigorous sub-Plinian and / or Plinian eruptions. Other mass-flow depositional series are rich in dense, glassy, monolithologic andesite clasts, corresponding to dome-building and associated block-and-ash-flow activity. Polyolithologic flows are probably not directly related to an eruption, but may represent conditions where mass-flows gained momentum via erosion and incorporation of sediment along their paths. The frequency, nature and volume of flows may also depend on the prevailing local and global climate, i.e. rainfall intensity and duration in the source region, vegetation patterns and related slope-stability or sediment supply (e.g. Lavigne et al., 2000; Waite et al., 1983; Mothes et al., 1998; Hodgson & Manville, 1999; Vallance, 2000; van Westen & Daag, 2005).

8.5. Distribution of deposits

The distribution of tephra is mainly controlled by the prevailing wind direction while that of flows depends strongly on the location of the source area (i.e. the direction of collapse or site of lahar initiation) and the nature of the landscape surrounding the volcano. A deeply incised topography leads to confinement of debris avalanches and lahars, as is the case at most

volcanoes in the Cascades, e.g. the Osceola Mudflow at Mt. Rainier (Vallance & Scott, 1997) and the 1980 debris avalanche at Mount St. Helens as well as subsequent lahars (Voight et al., 1981; Janda et al., 1981). In contrast, Mt. Taranaki debris avalanches form broad fans on the weakly dissected ring-plain. Through most of Taranaki's history the ring-plain setting resembled the present landscape, which is characterised by mostly shallow stream beds and wide coastal plains with broad terraces resulting in the predominance of relatively unconfined and extended sheet-like volcanic mass-flows. Some larger, long-lived river systems provided flow paths for channelised lahars but were commonly infilled and covered by sheet-like flows. Subsequent fluvial erosion again incised some valleys that formed new paths to guide younger flows (Procter et al., 2008, this volume). The thickness of mass-flows at any one location in Taranaki increased with growing height and volume of the edifice. In general, the travel-distance of lahars is expected to depend on the elevation and nature of the source region, origin of the flow, slope angle, type and grain-size of the transported material, sediment/water ratio as well as the volume of the flow (Fisher & Schmincke, 1984; Scott, 1988; Pierson et al. 1990; Mothes 1992; Scott et al., 1995; Vallance, 2000).

Mt. Taranaki debris avalanches form broad fans on the weakly dissected ring-plain (Neall et al., 1986; Palmer et al., 1991; Alloway et al., 2005) and their distribution is mainly controlled by the direction of collapse. Several models have tried to relate volcano morphology and the direction of edifice failures to the regional tectonic stress field. Nakamura (1977), Moriya (1980) and Siebert (1984) suggested that where volcanoes respond to an existing stress regime, the preferred orientation of the axis of the avalanche scarp is perpendicular to the regional σ_{Hmax} or to the strike of normal faults (Francis & Self, 1987). Second generation collapse events may be parallel to the previous axes, or at a high angle, i.e. c.135° (Siebert, 1984). Later studies showed that volcanoes respond in different ways to the tectonic stress and have varying orientations of amphitheatres in relation to σ_{Hmax} depending on their geodynamic setting (Lagmay & Valdivia, 2006). Failure directions were found to occur at an

angle to σ_{Hmax} with the highest frequency at 20°-30° and 40°-50° (Lagmay & Valdivia, 2006) and are mainly influenced by temporal and local stress-fields within the edifice (Ui et al., 1986b), the geometry and nature of faults (Tibaldi, 1995; Lagmay et al., 2000; Vidal & Merle, 2000) and the subvolcanic basement (van Wyk de Vries & Borgia, 1996; Wooller et al., 2004; Tibaldi et al., 2005). The NE-SW orientation of the numerous active and inactive Quaternary faults that cut the Taranaki peninsula (Fig. 1B) dates from the initial formation of the Tasman Sea c. 80 Ma ago (Hull & Dellow 1993) and does no longer reflect the current stress field (Sherburn & White 2006). The NNW-SSE alignment of the Taranaki volcanoes and the younger N-S trend of Mt. Taranaki and flank vents (Neall 1971) differ significantly from the NW-SE orientation of the observed faults, indicating that magmatic intrusions are responsible for the long-term change of the stress direction (Sherburn & White 2006). The distribution axes of debris avalanches at Mt. Taranaki are oriented at various angles to the main structural lineament, and the regional σ_{Hmax} without obvious pattern. Most probably the direction of collapse at Mt. Taranaki was influenced by the trigger mechanisms, i.e. magmatic intrusions / large-scale explosive eruptions and large fault movements in combination with the apparent structural alignments and the morphology of the edifice at the time of failure.

8.6. Sedimentation between eruptive episodes

The sedimentation as well as erosion and redeposition between eruptive episodes vary according to climate and setting as well as sediment supply. In south-west Taranaki, organic-rich soil and peat beds accumulated during warm periods, while loess-rich tephric soils formed in cooler climate. Fluvial erosion and reworking of primary deposits produced sediments ranging from localised cross-bedded, well-sorted sand and pebble beds to aggradational series of river gravel interbedded with lenses of fluvial sand. Some areas accumulated massive sequences of well-sorted dune sands due to near-shore aeolian

redeposition during periods of sea level high-stands. Interbedded coarser beds entirely made up of rounded pumice lapilli were formed shortly after eruptive episodes.

8.7. Hazard implications

Overall, the hazard potential varies strongly at different parts of the cycle, because each phase generates distinctive types of mass-flows. Although large edifice failures and the generation of debris avalanches individually represent the greatest hazard at repetitively collapsing volcanoes, they are usually of low frequency, i.e. on-average every 10 ka at Mt. Taranaki. During construction phases, eruption-related mass-flows are by far more frequent and are not only confined to stream valleys but can inundate wide areas and travel long distances. Large channelised debris flows occur at least once in c. 2 ka while sheet-like hyperconcentrated flows are the most frequent event recorded in medial ring-plain locations, with a minimum recurrence of one event in 500 years. Due to the large number and narrow distribution range of single flow units and the lack of individual diagnostic properties, hyperconcentrated flow and debris flow deposits were grouped into composite stratigraphic units and correlated as packages rather than separate flow events. The given frequency is thus only an approximate minimum estimate.

9. Conclusions

Edifice failures at Mt. Taranaki occurred on-average every 10 ka, with five collapses being recognised over the last 30 ka where stratigraphic records are more complete. The unstable nature of Mt. Taranaki is mainly a result of its weak internal structure and the characteristics of the subvolcanic basement. Large-scale edifice failures were most likely triggered by significant fault movements or associated with magmatic intrusions and / or major eruptions.

The volcanoclastic ring-plain succession surrounding Mt. Taranaki records these periods of destruction as well as other volcanic and sedimentary events of the last 130 ka. The variety of

different sediment lithofacies reflects a range of transport and emplacement modes as well as various depositional environments. The exposed volcanic mass-flow deposits were produced by a wide spectrum of sediment-water flow, ranging from granular debris avalanches and associated cohesive debris flows, non-cohesive channelised debris flows and related overbank hyperconcentrated flows to more dilute, sheet-like hyperconcentrated flows and normal stream flow.

The different facies are related to specific periods within a repeating pattern of deposition, which was here used to develop a model of cyclic volcanoclastic sedimentation at stratovolcanoes. Cyclic growth and collapse represent a natural frequency in the behaviour of long-lived andesitic stratovolcanoes, but are often difficult to identify because of the long time-scales of cycles or incomplete stratigraphic records. Individual volcanic cycles may vary in detail between different volcanoes and also during the life-time of a single volcano. Their characteristics are influenced by various internal and external factors, including frequency and nature of collapse events, duration and style of eruptive periods, as well as the surrounding topography and climate conditions.

Understanding the cyclic nature of stratovolcanoes and the frequency of their cyclicity will be critical for developing realistic probabilistic hazard models. The historic record can provide information on the nature, extent and recurrence of past collapse (and lahar) events while the nature of eruptive activity in the recent record can help to evaluate which part of the cycle the volcano is currently in and what hazards can be expected.

An almost completely regenerated edifice with steep upper slopes suggests that Mt Taranaki is close to the end of a volcanic cycle. Which type of hazard is most likely in the near future depends on the nature of potential internal and external processes, such as resuming eruptive activity, seismic events, intense rainstorms etc. Possible scenarios in Taranaki can cover the whole spectrum of volcanic and volcanoclastic events observed in the historic record of the

volcano, including lava flows, ash fall, pyroclastic flows, lahars or even edifice failure and the generation of a debris avalanche.

Acknowledgements

AVZ was supported by a Massey University and German Academic Exchange Service (DAAD) Doctoral Scholarship, and the George Mason Trust. SJC and JNP are supported by the NZ FRST contract MAUX0401. We are grateful to B. van Wyk de Vries and A. Draut for constructive reviews of an earlier version of this manuscript and B. van Wyk de Vries and A. Szakács for further helpful suggestions on this version. Thanks also to RB Stewart for helpful discussions.

References

- Alloway, B., 1989. Late Quaternary cover-bed stratigraphy and tephrochronology of north-eastern and central Taranaki, New Zealand. Ph.D. thesis, INR, Massey University, Palmerston North, New Zealand, 406 pp.
- Alloway, B.V., Neall, V.E., Vucetich, C.G., 1995. Late Quaternary tephrostratigraphy of north-east and central Taranaki, J. Roy. Soc. NZ 25, 385-458.
- Alloway, B., McComb, P., Neall, V., Vucetich, C., Gibb, J., Sherburn, S., Stirling, M., 2005. Stratigraphy, age, and correlation of voluminous debris avalanche events from an ancestral Egmont Volcano: implications for coastal plain construction and regional hazard assessment. J. Roy. Soc. NZ 35, 229-267.
- Beget, J.E., Kienle, J., 1992. Cyclic formation of debris avalanches at Mount St Augustine volcano. Nature 356, 701-704.
- Belousov, A., Belousova, M., Voight, B., 1999. Multiple edifice failures, debris avalanches and associated eruptions in the Holocene history of Shiveluch volcano, Kamchatka, Russia. Bull. Volcanol. 61, 324-342.

- Bogoyavlenskaya, G.E., Braitseva, O.A., Melekestsev, I.V., Kiriyanov, V.Yu., Miller, C.D., 1985. Catastrophic eruptions of the directed-blast type at Mount St. Helens, Bezymianny and Shiveluch volcanoes. *J. Geod.* 3, 189-218.
- Borgia, A., 1994. The dynamic basis of volcano spreading. *J. Geophys. Res.*, 99, 17791-17804.
- Borgia, A., van Wyk de Vries, B., 2003. The volcano-tectonic evolution of Concepcion, Nicaragua. *Bull. Volcanol.* 65, 248-266.
- Capra, L., 2006. Abrupt climatic changes as triggering mechanisms of massive volcanic collapses. *J. Volcanol. Geoth. Res.* 155, 329-333.
- Capra, L., Macias, J.L., Scott, K.M., 2002. Debris avalanches and debris flows transformed from collapses in the Trans-Mexican Volcanic Belt, Mexico behaviour, and implications for hazard assessment. *J. Volcanol. Geoth. Res.* 113, 81-110.
- Carracedo, J.-C., 1994. The Canary Islands: an example of structural control on the growth of large oceanic-island volcanoes. *J. Volcanol. Geoth. Res.* 60, 225-241.
- Carracedo, J.-C., 1996. A simple model for the genesis of large gravitational landslide hazards in the Canary Islands. In: McGuire, W.J., Jones, A.P., Neuberg, J. (Eds.), *Volcano Instability on the Earth and other planets*. Geol. Soc. London Spec. Publ. 110, 125-136.
- Carrasco-Núñez, G., Díaz-Castellón, R., Siebert, L., Hubbard, B., Sheridan, M.F., Rodríguez, S.R., 2006. Multiple edifice-collapse events in the Eastern Mexican Volcanic Belt: The role of sloping substrate and implications for hazard assessment. *J. Volcanol. Geoth. Res.* 158, 151-176.
- Concha-Dimas, A., Cerca, M., Rodríguez, S.R., Watters, R.J., 2005. Geomorphological evidence of the influence of pre-volcanic basement structure on emplacement and deformation of volcanic edifices at the Cofre de Perote-Pico de Orizaba chain and implications for avalanche generation. *Geomorphology* 72, 1-4.

- Crandell, D.R., Miller, C.D., Glicken, H.X., Christiansen, R.L., Newhall, C.G., 1984. Catastrophic debris avalanche from ancestral Mount Shasta Volcano, California. *Geology* 12, 143-146.
- Cronin, S.J., Neall, V.E., Palmer, A.S., 1996. Geological history of the northeastern ring plain of Ruapehu volcano, New Zealand. *Quat. Int.* 35, 21-28.
- Cronin, S.J., Neall, V.E., Lecointre, J.A., Palmer, A.S., 1997. Changes in Whangaehu River lahar characteristics during the 1995 eruption sequence, Ruapehu volcano, New Zealand. *J. Volcanol. Geoth. Res.* 76, 47-61.
- Cronin, S.J., Neall, V.E., Lecointre, J.A., Palmer, A.S., 1999. Dynamic interactions between lahars and stream flow: a case study from Ruapehu volcano, New Zealand. *Geol. Soc. Am. Bull.* 111, 28-38.
- Cronin, S.J., Lecointre, J.A., Palmer, A.S., Neall, V.E., 2000. Transformation, internal stratification, and deposition of a channelised, multi-peaked lahar flow. *NZ J. Geol. Geophys.* 43, 117-128.
- Davidson, J.P., De Silva, S., 2000. Composite volcanoes. In: *Encyclopedia of Volcanoes*, Eds H. Sigurdsson, B. Houghton, S. McNutt, H. Rymer, J. Stix., Academic Press, San Diego, p. 663-681.
- Donoghue, S.L., Neall, V.E., 2001. Late Quaternary constructional history of the southeastern Ruapehu ring plain, New Zealand. *NZ J. Geol. Geophys.* 44, 439-466.
- Elsworth, D., Voight, B., 1996. Evaluation of volcano flank instability triggered by dyke intrusion. In: McGuire, W.J., Jones, A.P., Neuberg, J. (Eds.), *Volcano Instability on the Earth and other planets*. *Geol. Soc. London Spec. Publ.* 110, 45-54.
- Firth, C., Stewart, I., McGuire, W., Kershaw, S., Vita-Finzi, C., 1996. Costal elevation changes in eastern Sicily: implications for volcano instability. In: McGuire, W.J., Jones, A.P., Neuberg, J. (Eds.), *Volcano Instability on the Earth and other planets*. *Geol. Soc. London Spec. Publ.* 110, 153-168.

- Fisher, R.V., Schmincke, H.-U., 1984. Pyroclastic rocks. Springer, Heidelberg, 472 p.
- Fornari, D.J., Campbell, J.F., 1987. Submarine topography around the Hawaiian Islands. US Geol. Surv. Prof. Pap. 1350, 109-124.
- Francis, P., Self, S., 1987. Collapsing volcanoes. *Sci. Am.* 256, 72-90.
- Gaylord, D.R., Neall, V.E., Palmer, A.S., 1993. The Maitahi Formation, A Mid-Pleistocene volcanic debris avalanche assemblage, Taranaki, New Zealand. Abstract in: Volcanic activity and the environment, abstracts of the IAVCEI, Puerto Vallarta, Mexico 1997 General Assembly. Gobierno de Jalisco, Unidad Editorial, Guadalajara, Mexico.
- Glicken, H., 1996. Rockslide-debris avalanche of May 18, 1980, Mount St. Helens volcano, Washington. US Geol. Surv., Open File Report 96-677, 90 pp.
- Grant-Taylor, T.L., Rafter, T.A., 1963. New Zealand natural radiocarbon measurements I-V. *Radiocarbon* 5, 118-162.
- Hodgson, K.A., Manville, V.R., 1999. Sedimentology and flow behaviour of a rain-triggered lahar, Mangatoetoe Stream, Ruapehu volcano, New Zealand. *Geol. Soc. Am. Bull.* 5, 743–754.
- Holcomb, R.T., Searle, R.C., 1991. Large landslides from oceanic volcanoes. *Marine Geotechnology* 10, 19-32.
- Hull, A.G., Dellow, G., 1993. Earthquake hazards in the Taranaki region. Institute of Geological & Nuclear Sciences Client Report 1993/03, Wellington.
- Janda, R.J., Scott, K.M., Nolan, K.M., Martinson, H.A., 1981. Lahar movement, effects, and deposits. In: Lipman, P.W., Mullineaux, D.R. (Eds.), *The 1980 eruptions of Mount St. Helens, Washington*. US Geol. Surv. Prof. Pap. 1250, 461-478.
- Kamp, P.J.J., Vonk, A.J., Bland, K.J., Hansen R.J., Hendy, A.J.W., McIntyre, A.P., Ngatai, M., Cartwright, S.J., Hayton, S., Nelson, C.S., 2004. Neogene stratigraphic architecture and tectonic evolution of Wanganui, King Country, and eastern Taranaki Basins, New Zealand. *NZ J. Geol. Geophys.* 47, 625-644.

- Kokelaar, P., Romagnoli, C., 1995. Sector collapse, sedimentation, and clast population evolution at an active island-arc volcano: Stromboli, Italy. *Bull. Volcanol.* 57, 240-161.
- Labazuy, P., 1996. Recurrent landsliding events on the submarine flank of Piton de la Fournaise volcano, Reunion Island. In: McGuire, W.J., Jones, A.P., Neuberg, J. (Eds.), *Volcano Instability on the Earth and other planets*. Geol. Soc. London Spec. Publ. 110, 293-306.
- Lagmay, A.M.F., van Wyk de Vries, B., Kerle, N., Pyle, D.M., 2000. Volcano instability induced by strike-slip faulting. *Bull. Volcanol.* 62, 331-346.
- Lagmay, A.M.F., Valdivia W., 2006. Regional influence on the opening direction of crater amphitheatres in Southeast Asian volcanoes. *J. Volcanol. Geoth. Res.* 158, 139-150.
- Lavigne, F., Thouret, J.-C., Voight, B., Suwa, H., Sumaryono, A., 2000. Lahars at Merapi volcano, Central Java: an overview. *J. Volcanol. Geoth. Res.* 100, 423–456.
- Lenat, J.F., Vincent, P., Bachelery, P., 1989. The off-shore continuation of an active basaltic volcano: Piton de la Fournaise, Reunion Island, Indian Ocean.; structural and geomorphological interpretation from sea beam mapping. *J. Volcanol. Geoth. Res.* 36, 1-36.
- Lipman, P.W., Mullineaux, D.R. (Eds.), 1981, *The 1980 eruptions of Mount St. Helens, Washington*. US Geol. Surv. Prof. Pap., 1250, 844 pp.
- Lopez, D., Williams, S., 1993. Catastrophic volcano collapse: relation to hydrothermal alteration. *Science* 260, 1794-1796.
- McGlone, M.S., Neall, V.E., Pillans, B.J., 1984. Inaha Terrace deposits: a late Quaternary terrestrial record in South, New Zealand. *NZ J. Geol. Geoph.* 27, 35-49.
- McGuire, W.J., 2003. Volcanic instability and lateral collapse. *Revista* 1, 33-45.
- Moore, J.G., Normark, W.R., and Holcomb, R.T., 1994. Giant Hawaiian Landslides. *Annu. Rev. Earth Planet. Sci.* 22, 119-144.
- Moriya, I., 1980. Bandaian eruption and landforms associated with it. *Collection of articles in memory of retirement of Prof. Hishimura*, 66. Tohoku University, Tokyo, 214-219.

- Mothes, P.A., 1992. Lahars of Cotopaxi Volcano, Ecuador: hazard and risk evaluation. In: McCall, G.J.H., Laming, D.J.C., Scott, S.C. (Eds.), *Geohazards, natural and man-made*. Chapman and Hall, London, p 53–63.
- Mothes, P.A., Hall, M.L., Janda, R.J., 1998. The enormous Chillos Valley Lahar: an ash-flow-generated debris flow from Cotopaxi Volcano, Ecuador. *Bull. Volcanol.* 59, 233-244.
- Murray, J., 1988. The influence of loading by lavas on siting of volcanic eruption vents on Mount Etna. *J. Volcanol. Geoth. Res.* 35, 121-139.
- Nakamura, K., 1977. Volcanoes as possible indicators of tectonic stress. *J. Volcanol. Geoth. Res.* 2, 1-16.
- Neall, V.E., 1971. Volcanic domes and lineations in Egmont National Park. *NZ J. Geol. Geoph.* 14, 71-81.
- Neall, V.E., 1979. Sheets P19, P20 and P21 New Plymouth, Egmont and Manaia, Geological Map of New Zealand. NZ Dep. Sci. Ind. Res., Wellington, scale 1:50 000, 3 sheets, 36 pp.
- Neall, V.E., Stewart, R.B., Smith, I.E.M., 1986. History and petrology of the Taranaki volcanoes. *Roy. Soc. NZ Bull.* 23, 251-263.
- Palmer, B.A., Neall, V.E., 1991. Contrasting lithofacies architecture in ring-plain deposits related to edifice construction and destruction, the Quaternary Stratford and Opunake Formations, Egmont Volcano, New Zealand. *Sed. Geol.* 74, 71-88.
- Palmer, B.A., Alloway, B.V., Neall, V.E., 1991. Volcanic-debris-avalanche deposits in New Zealand - lithofacies organisation in unconfined, wet-avalanche flows. In: Fisher, R.V., Smith, G.A. (Eds.), *Sedimentation in Volcanic Settings*. SEPM Spec. Pub. 45, 89-98.
- Pierson, T.C., Scott, K.M., 1985. Downstream dilution of a lahar: transition from debris flow to hyperconcentrated streamflow. *Water Resour. Res.* 21, 1511–1524.
- Pierson, T.C., Janda, R.J., Thouret, J.C., Borrero, C.A., 1990. Perturbation and melting of snow and ice by the 13 November 1985 eruption of Nevado del Ruiz, Colombia and

consequent mobilization, flow, and deposition of lahars. *J. Volcanol. Geotherm. Res.* 41, 17-66.

Pillans, B., 1983. Upper Quaternary marine terrace chronology and deformation, South Taranaki, New Zealand. *Geology* 11, 292-297.

Pillans, B., 1994. Direct marine-terrestrial correlations, Wanganui Basin, New Zealand: The last 1 million years. *Quat. Sci. Rev.* 13, 189-200.

Platz, T., Cronin, S.J., Cashman, K.V., Stewart, R.B., Smith, I.E.M., 2007. Transitions from effusive to explosive phases in andesite eruptions - a case-study from the AD1655 eruption of Mt. Taranaki, New Zealand. *J. Volcanol. Geoth. Res.* 161, 15-34.

Price, R.C., Stewart, R.B., Woodhead, J.D., Smith, I.E., 1999. Petrogenesis of High-K Arc Magmas: Evidence from Egmont Volcano, North Island, New Zealand. *J. Petrol.* 40, 167-197.

Procter, J.N., Cronin, S.J., Zernack, A.V., 2008. Landscape and sedimentary response to catastrophic debris avalanches, western Taranaki, New Zealand. In: Nemeth, K., Manville, V., Kano, K. (Eds.), *Source to sink: from volcanic eruptions to volcanoclastic deposits on the Pacific Rim*. [this volume]

Reid, M.E., Sisson, T.W., Brien, D.L., 2001. Volcano collapse promoted by hydrothermal alteration and edifice shape, Mount Rainier, Washington. *Geology* 29, 779-782.

Scott, K.M., 1988. Origin, behaviour, and sedimentology of lahars and lahar-runout flows in the Toutle-Cowlitz river system. *US Geol. Surv. Prof. Pap.* 1447, 74 pp.

Scott, K.M., Vallance, J.W., Pringle, P.T., 1995. Sedimentology, behaviour, and hazards of debris flows at Mount Rainier, Washington. *US Geol. Surv. Prof. Pap.* 1547, 56 pp.

Scott, W.E., Pierson, T.C., Schilling, S.P., Costa, J.E., Gardner, C.A., Vallance, J.W., Major, J.J., 1997. Volcano hazards in the Mount Hood region, Oregon. *U.S. Geol. Surv. Open-File Report* 97-89, 14 pp.

- Scott, K., Vallance, J., Kerle, M., Macías, J.L., Strauch, W., Devoli, G., 2005. Catastrophic precipitation-triggered lahar at Casita volcano, Nicaragua; occurrence, bulking and transformation. *Earth Surf. Proc. Land.* 30, 59-79.
- Shea, T., van Wyk de Vries, B., Pilato, M., 2008. Emplacement mechanisms of contrasting debris avalanches at Volcán Mombacho, Nicaragua., provided by structural and facies analysis. *Bull. Volc.*, DOI 10.1007/s00445-007-0177-7.
- Sherburn, S., White, R.S., 2006. Tectonics of the Taranaki region, New Zealand: earthquake focal mechanisms and stress axes. *NZ J. Geol. Geophys.*, 49, 269-279.
- Siebert, L., 1984. Large volcanic debris avalanches: characteristics of source areas, deposits and associated eruptions. *J. Volcanol. Geoth. Res.* 22, 163-197.
- Siebert, L., Beget, J.E., Glicken, H., 1995. The 1883 and late-prehistoric eruptions of Augustine volcano, Alaska. *J. Volcanol. Geoth. Res.* 66, 367-395.
- Smith, G.A., 1987. The influence of explosive volcanism on fluvial sedimentation: The Deschutes Formation, Neogene. in central Oregon. *J. Sed. Petrol.* 57, 613-629.
- Smith, G.A., 1991. Facies Sequences and geometries in continental volcanoclastic settings. In: Fisher, R.V., Smith, G.A. (Eds.), *Sedimentation in Volcanic Settings*. SEPM Spec. Publ. 45, 109-121.
- Stoopes, G.R., Sheridan, M.F., 1992. Giant debris avalanches from the Colima Volcanic Complex, Mexico: Implication for long-runout landslides, >100 km. *Geology* 20, 299-302.
- Thouret, J.-C., Cantagrel, J.-M., Robin, C., Murcia, A., Salinas, R., Cepeda, H., 1995. Quaternary eruptive history and hazard-zone model at Nevado de Tolima and Cerro Machin Volcanoes, Colombia. *J. Volcanol. Geotherm. Res.* 66, 397-426.
- Tibaldi, A., 1995. Morphology of pyroclastic cones and tectonics. *J. Geophys. Res.* 100, 24521-24535.
- Tibaldi, A., 2001. Multiple sector collapses at Stromboli volcano Italy: how they work. *Bull. Volcanol.* 63, 112-125.

- Tibaldi, A., Lagmay, A.M.F., Ponomareva, V., 2005. Effects of basement structural and stratigraphic heritages on volcano behaviour and implications for human activities. *Episodes* 28, 158-170.
- Ui, T., Kawachi, S., Neall, V.E., 1986a. Fragmentation of debris avalanche material during flowage - evidence from the Pungarehu Formation, Mount Egmont, New Zealand. *J. Volcanol. Geoth. Res.* 27, 255-264.
- Ui, T., Yamamoto, H., Suzuki-Kamata, K., 1986b. Characterisation of debris avalanche deposits in Japan. *J. Volcanol. Geoth. Res.* 29, 231-243.
- Vallance, J.W., Scott, K.M., 1997. The Osceola Mudflow from Mount Rainier; sedimentology and hazard implications of a huge clay-rich debris flow. *GSA Bull.* 109, 143-163.
- Vallance, J.W., Siebert, L., Rose, W.I. Jr., Giron, J.R., Banks, N.G., 1995. Edifice collapse and related hazards in Guatemala. *J. Volcanol. Geoth. Res.* 66, 337-355.
- Vallance, J.W., 2000. Lahars. In: Sigurdsson, H., Houghton, B., McNutt, S., Rymer, H., Stix, J. (Eds.), *Encyclopedia of Volcanoes*. Academic Press, San Diego, pp. 601-616.
- Van Westen, C.J., Daag, A.S., 2005. Analysing the relation between rainfall characteristics and lahar activity at Mount Pinatubo, Philippines. *Earth Surf. Proc. Land.* 30, 1663-1674.
- Van Wyk de Vries, B., Borgia, A., 1996. The role of basement in volcano deformation. In: McGuire, W.J., Jones, A.P., Neuberg, J. (Eds.), *Volcano Instability on the Earth and other planets*. *Geol. Soc. London Spec. Publ.* 110, 95-110.
- Van Wyk de Vries, B., Francis, P., 1997. Catastrophic collapse at stratovolcanoes induced by gradual volcano spreading. *Nature* 387, 387-390.
- Van Wyk de Vries, B., Kerle, N., Petley, D., 2000. Sector collapse forming at Casita volcano, Nicaragua. *Geology* 28, 167-170.
- Van Wyk de Vries, B., Self, S., Francis, P.W., Keszthely, L., 2001. A gravitational spreading origin for the Socompa debris avalanche. *J. Volcanol. Geoth. Res.* 105, 225-247.

- Vidal, N., Merle, O., 2000. Reactivation of basement faults beneath volcanoes: a new model for flank collapse. *J. Volcanol. Geoth. Res.* 99, 9-26.
- Voight, B., Glicken, H., Janda, R.J., Douglass, P.M., 1981. Catastrophic rockslide avalanche of May 18. In: Lipman, P.W. Mullineaux, D.R. (Eds.), *The 1980 eruptions of Mount St. Helens*, Washington. US Geol. Surv. Prof. Pap. 1250, 347-377.
- Voight, B., Elsworth, D., 1997. Failure of volcano slopes. *Geotechnique* 47, 1-31.
- Waitt, R.B. Jr., Pierson, T.C., MacLeod, N.S., Janda, R.J., Voight, B., Holcomb, R.T., 1983. Eruption-triggered avalanche, flood and lahar at Mount St. Helens: effects of winter snowpack. *Science* 22, 1394–1397.
- Walter, T.R., Schmincke, H.-U., 2002. Rifting, recurrent landsliding and Miocene structural reorganization on NW-Tenerife, Canary Islands. *Int. J. Earth Sci.* 91, 615-628.
- Waythomas, C.F., 1999. Stratigraphic framework of Holocene volcanoclastic deposits, Akutan Volcano, east-central Aleutian Islands, Alaska. *Bull. Volcanol.* 61, 141-161.
- Waythomas, C.F., Miller, T.P., 1999. Preliminary volcano-hazard assessment for Iliamna Volcano, Alaska. U.S. Geol. Surv. Open-File Report 99-373, 31 pp.
- Waythomas, C.F., Wallace, K.L., 2002. Flank collapse at Mount Wrangell, Alaska, recorded by volcanic mass-flow deposits in the Copper River lowland. *Can. J. Earth Sci.* 39, 1257-1279.
- Wooller, L., van Wyk de Vries, B., Murray, J.B., Rymer, H., Meyer, S., 2004. Volcano spreading controlled by dipping substrata. *Geology* 32, 573-576.

Tables

Table 1. Overview of some aspects of Mt. Taranaki debris avalanche deposits.

Debris avalanche unit	Direction of collapse	Age (ka)	Max. medial thickness (m)	Max. observed medial width (km)	Runout (km)
Opua	SW	6.6 ^a	8	25	27+
Motumate	S	10-14 ^b	3.5	10.8	31+
Pungarehu	W	20 ^c	>16	35	26+
Ngaere	SE	23 ^d	5	>11	34+
Te Namu	SW	29 ^c	>5	>9	26+
Rama	S	>35 ^{ce}	12	25.5	34+
Otakeho	S	>50 ^c	>4	24.5	32+
Tokaora	S	c.60 ^b	2.5	2	35+
Waihi	S	c.70 ^b	8	17.8	45+
Waingongoro	S	c.75 ^b	5	16.6	44+
Oeo	S	>80 ^{bf}	>6	>21	34+
Okawa	NE	c.105 ^d	4	9	39+
Motunui	NE	>130 ^d	6	17	41+
Mangati ^g	NE	>190 ^b	6	?	39+

^a Neall et al. (1986).

^b Chronostratigraphy this study.

^c Radiocarbon dating this study (cf. Table 2).

^d Alloway et al. (2005).

^e Radiocarbon date NZ-331 (Grant-Taylor & Rafter, 1963)

^f Racemisation age BJB-010 (McGlone et al., 1984)

^g Debris avalanche deposit most likely derived from Mt. Taranaki.

Table 2. Overview of radiocarbon analytical data obtained for selected Taranaki debris avalanche deposits.

Debris avalanche unit	Sample number	Sample type, stratigraphic position	Laboratory number	Analysis method	Radiocarbon Age (BP)	Inferred DAD age (ka)
Pungarehu	AZ05-D01	Peat directly below DAD	Wk-16398/ NZA-22349	AMS	20,776 ± 170	<20.8
Te Namu	AZ05-D11	Organic soil above DAD	Wk-16401	LSC	25,198 ± 167	>25.2
	AZ05-D14b	Tree log from DAD	Wk-16402/ NZA-22895	AMS	29,074 ± 399	<29.1
Rama	AZ06-D06	Thick peat above DAD	Wk-19143	LSC	28,824 ± 237	>28.8
Otakeho	AZ06-D01	Wood from DAD	Wk-19140	LSC	background	>50
Oeo	AZ06-D02	Large log from DAD	Wk-19141	LSC	background	>50

Table 3. Sedimentary characteristics and distinction criteria of different types of observed volcanic mass-flow, fluvial and aeolian deposits.

Deposit type	Sedimentary characteristics	Contacts and geometry
Cohesive debris flow deposits	<p>Matrix-supported</p> <p>Pebble- to boulder-sized clasts in a clay-rich matrix</p> <p>Extremely poorly to very poorly sorted</p> <p>Massive, unstratified</p> <p>Typically ungraded, some deposits with coarse basal layer</p> <p>Shattered and fractured clasts, brecciated and stratified megaclasts, rip-up clasts, ripped-up wood</p> <p>Typically 4-6m thick, maximum up to 10m thick</p>	<p>Non-erosive, draping of irregularities</p> <p>Unconfined fan</p>
Non-cohesive debris flow deposits	<p>Matrix-supported</p> <p>Pebble- to boulder-sized clasts in a sandy matrix</p> <p>Very poorly to poorly sorted</p> <p>Massive, unstratified</p> <p>Ungraded or reverse-to-normal grading</p> <p>Typically 0.4-0.6 m but up to 1.7 m thick</p> <p>Deposits often reflect transformation of debris to hyperconcentrated flow: they consist of an inversely graded, fine-grained layer with horizontal fabric and a coarse, massive, poorly sorted breccia unit that grades into a finer-grained, bedded top part</p>	Typically tabular, non-erosive, some lenticular with scoured basal contacts
Channelised debris flow and associated overbank deposits	<p>Clast-supported with little sandy matrix</p> <p>Very coarse, pebble to boulder-sized clasts</p> <p>Very poorly to extremely poorly sorted</p> <p>Massive, lack of internal stratification but often show a thin matrix-supported base</p> <p>Non-graded</p> <p>Up to 5 m thick</p> <p>Often upward transition to bedded, sandy deposits with weak horizontal fabric (hyperconcentrated flow)</p> <p>Intercalated lenses of cross-bedded and well sorted sands (fluvial) due to rapid post-depositional reworking</p> <p>Fine pebbly sands but coarser near channel</p> <p>Poorly sorted near channel, becoming moderately to well-sorted with distance from channel margins</p> <p>Faint internal stratification near channel, becoming progressively more distinct with thin horizontal and often very low-angle cross beds near the deposit margin</p> <p>Ungraded</p> <p>Up to 2 m thick but pinch out over 20 to 250 m from the channel margins</p>	<p>Erosive basal and marginal contacts</p> <p>Channel-confined, several tens of metres wide, lateral transition to overbank deposits</p> <p>Non-erosive</p> <p>Wedge-shaped, extend up to 250 m from channel margins</p>
Sheet-like hyperconcentrated flow deposits	<p>Pebbly sands, isolated pebble- to cobble-sized clasts, predominantly monolithologic components</p> <p>Poorly to moderately sorted</p> <p>Massive or bedded</p> <p>Reverse-to-normal grading, normal grading or no grading</p> <p>Typically 0.2-0.5 m thick, up to 2 m faintly bedded coarser units, up to 1.2 m well-bedded fine-grained units</p> <p>Occurrence of pumice ‘trains’ and aligned clasts</p> <p>Post-depositional deformation and dewatering structures (flame and dish and pillar structures)</p>	<p>Typically non-erosive, more dilute units lenticular with erosive basal contacts</p> <p>Sheets, up to 2.5 km wide</p>

Transitional hyperconcentrated flow / stream flow deposits	Fine- to coarse-grained sands	Erosive, wavy basal contacts
	Moderately to well-sorted Horizontal bedding to low-angle cross-bedding, lenses of cross-bedded fine sands and pebbles Ungraded Few-cm to 0.5 m thick units	Lenticular, often steep, overlapping channels
Normal stream flow deposits	Clast-supported	Erosive
	Fine to coarse sands, sands and rounded pebbles, pebble- to boulder-sized rounded clasts Well to moderately sorted in individual beds, poor sorting of aggradational deposit series Horizontal lamination of sands, low-angle cross-stratification and prominent scour-fill cross-bedding of alternating thin lenses (few mm to 1 cm thick) of well-sorted sands and beds (1 to 10 cm thick) of moderately to poorly sorted pebbles and sands Massive to faintly bedded aggradational sequences of silts and sands with intercalated cross-bedded lenses of fine pebbles and sand Up to 4 m-thick sequences of alternating sandy and pebbly beds, >10 m thick aggradational series	Lenticular Complex sequences of overlapping channels up to 150 m wide
Aeolian deposits	Grain-supported	Non-erosive
	Fine dark grey and coarse light yellow to brownish sands Well to very well-sorted Planar or high-angle cross-stratification of alternating thin (0.5-1 cm) beds of fine sands and thicker (up to 2 cm) beds of coarser sands Tens of cm to c. 1.5 m thick individual sets of dune sands, sequences up to 12 m thick	Extensive sand dune fields

Figure Captions

Figure 1:

- A) Overview map of the North Island, New Zealand, and major late Quaternary volcanic areas
- B) Geological map of the Taranaki Peninsula showing the setting of the Taranaki volcanic lineament and the distribution of different types of deposits (after Neall, 1979; Alloway *et al.*, 2005). The extent of the Mt. Taranaki ring plain is indicated in grey. Important sites discussed below are marked by stars.
- C) DEM of the Taranaki Peninsula showing the topography of the ring plain, the location of the study area and major faults (after Neall, 1979; Alloway *et al.*, 2005).
- D) View of the Taranaki volcanoes from the west, with Pouakai volcano to the north and Mt. Taranaki and the satellite vent Fanthams Peak to the south.
- E) View of Mt. Taranaki from the northwest showing the shape of the edifice with steep upper slopes and mounds of the Pungarehu debris avalanche deposit in the foreground.

Figure 2: Debris avalanche deposits of the granular-type in Axial-B and marginal facies.

- A) Coarse, massive fabric of Axial-B debris avalanche deposit. Hammer is 30 cm long.
- B) Fractured clast
- C) Large megaclast in Axial-B facies, c. 50 m across.
- D) Small brecciated megaclast
- E) Rip-up clast of hyperconcentrated flow deposit
- F) Basal layer with pebble- to boulder-sized clasts

Figure 3: Debris avalanche and debris flow deposits of the cohesive type in marginal facies.

- A) Fabric of matrix-rich, cohesive debris flow deposit.
- B) Ripped-up fragments of wood and underlying soil.
- C) Small rounded megaclast.

D) Stratified rip-up clast of peat and tephra layers.

Figure 4: Channelised debris flow and related overbank deposits.

- A) Coarse bouldery channelised debris flow deposit
- B) Coarse debris flow deposit filling a steep channel with lateral transition to overbank facies
- C) Wide channel filled by a coarse debris flow deposit that grades into finer-grained and better sorted overbank hyperconcentrated flow deposits

Figure 5: Different lithology assemblages within sheet-like hyperconcentrated flow deposits.

- A) Pumiceous monolithologic type
- B) Dense monolithologic type.
- C) Polyolithologic type.

Figure 6: Sedimentary features of hyperconcentrated flow deposits.

- A) Reverse to normal grading in deposits produced by transitional debris to hyperconcentrated flows.
- B) Massive, ungraded, 1 m thick hyperconcentrated flow deposit.
- C) Crudely bedded hyperconcentrated flow deposit in the middle of the picture underlain by finer-grained hyperconcentrated flow deposit with coarser clasts aligned parallel to depositional surface.
- D) Small pumice clasts clustered in front of a larger clast.
- E) Flame loading structures.
- F) Dish and pillar dewatering structures.

Figure 7: Transitional hyperconcentrated - stream flow deposits with bedding features.

- A) Thin horizontal to wavy bedding.

- B) Lenticular cross-bedded deposits produced by transitional hyperconcentrated to stream flow, forming a sequence of overlapping small channels.

Figure 8: Fluvial deposits and bedding features.

- A) Localised planar and ripple cross-bedded fluvial deposits.
- B) Bedded and cross-bedded river gravel and sands, pen for scale (15 cm long).
- C) Thick sequence of trough and planar cross-bedded fluvial sands and pebbles.
- D) Aggradational river gravels and sands with intercalated lenses of cross-bedded sands.

Figure 9: Aeolian deposits and bedding features.

- A) High-angle cross-stratification in fine-grained, well-sorted dune sands overlain by more massive sands.
- B) Thick sequence of planar and high-angle cross-bedded dune sands.

Figure 10: Representative ring-plain sections in Taranaki showing the different types of lithofacies associations. Locations are marked in Fig. 1.

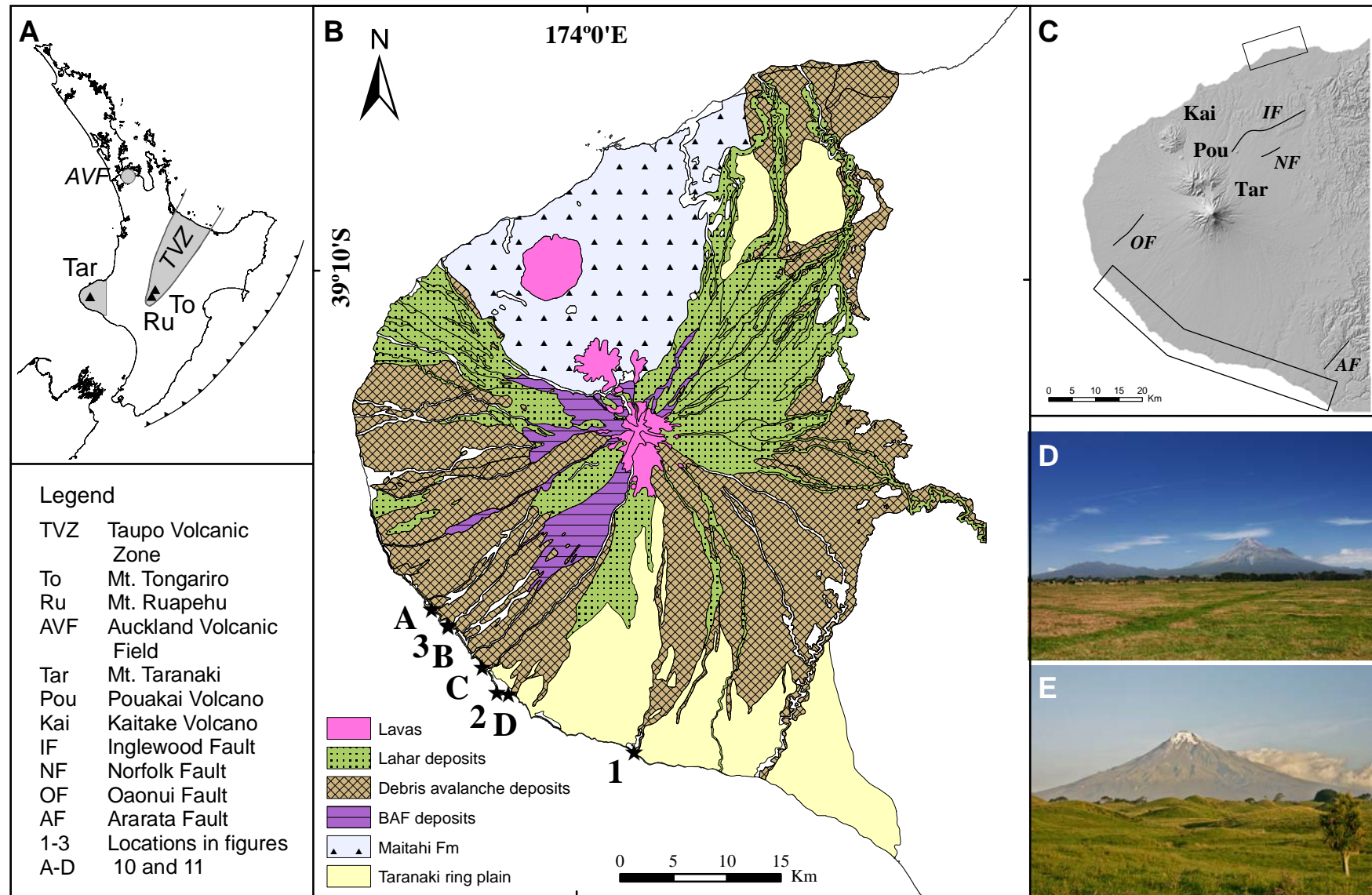
- A) Deposit sequence 1 (Kaupokonui) includes two massive debris-avalanche deposits (DAD), which are separated by hyperconcentrated-flow (HFD) and debris-flow (DFD) units and underlain by alternating hyperconcentrated-flow and fluvial (Flu) deposits.
- B) Deposit sequence 2 (Puketapu) consists of a paleo-channel filled by confined coarse debris-flow deposits (CH) that are overlain by sheet-like hyperconcentrated flow and fluvial deposits.
- C) Deposit sequence 3 (Opunake) is made up of stacked hyperconcentrated-flow units and a marginal debris avalanche deposit.

Figure 11: Examples of volcanoclastic sequences along the Taranaki coast, locations are marked in Fig. 1. Stratigraphic columns B-D represent examples of accumulation between collapse events.

- A) Debris-avalanche dominated sequence, here characterised by three massive debris avalanche units with interbedded soil / peat and tephra layers that represent accumulation between collapse events.
- B) Paleo-channel system filled by debris flow and hyperconcentrated flow deposits.
- C) Sequence dominated by sheet-flow deposits, here interbedded with fluvial sediments and soil / ash layers.
- D) Aeolian redeposited dune sands separated by thin soil / peat beds and individual hyperconcentrated flow deposits.

Figure 12: Simplified model of cyclic behaviour of stratovolcanoes in general and associated volcanic and volcanoclastic sedimentation as observed at Mt. Taranaki.

Fig. 1

















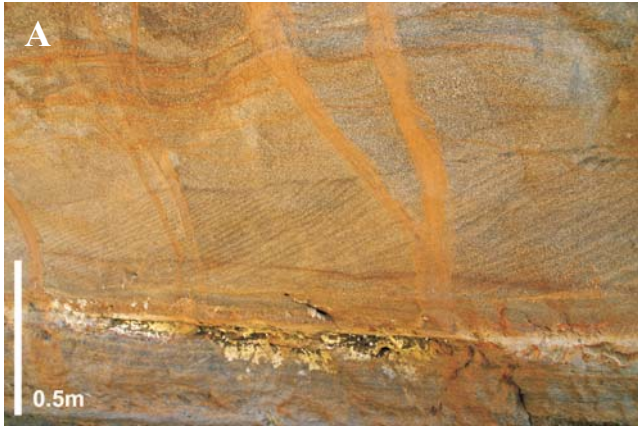




Fig. 11

